Click Here for Full Article

GOES sounding improvement and applications to severe storm nowcasting

Zhenglong Li,[1] Jun Li,[1] W. Paul Menzel,[1] Timothy J. Schmit,[2] James P. Nelson III,[1] Jaime Daniels,[2] and Steven A. Ackerman[1]

Received 26 November 2007; accepted 3 January 2008; published 6 February 2008.

[1] An improved clear-sky physical retrieval algorithm for atmospheric temperature and moisture is applied to the Geostationary Operational Environmental Satellite-12 (GOES-12) Sounder. A comparison with the microwave radiometer (MWR) measured total precipitable water (TPW) at the Southern Great Plains (SGP) Cloud and Radiation Testbed (CART) site from June 2003 to May 2005 shows that the TPW retrievals are improved by 0.4 mm over the legacy GOES Sounder TPW product. The Lifted Index (LI) derived product imagery (DPI) from the improved soundings better depicts the pre-convective environment surrounding a tornadic supercell at Eagle Pass, Texas on 24 April 2007. Another severe storm case from 13 April 2006 demonstrates that the improved physical algorithm successfully detects low-level moisture. Both cases show the new retrievals along with the derived products will help the forecasters with short-term severe storm nowcasting. **Citation:** Li, Z., J. Li, W. P. Menzel, T. J. Schmit, J. P. Nelson III, J. Daniels, and S. A. Ackerman (2008), GOES sounding improvement and applications to severe storm nowcasting, *Geophys. Res. Lett.*, *35*, L03806, doi:10.1029/2007GL032797.

1. Introduction

[2] Since 1994 the GOES Sounders (GOES-8/9/10/11/12/13) have been measuring radiances in 18 infrared (IR) spectral bands, ranging from approximately 3.7 to 14.7 μm, on an hourly basis over North America and adjacent oceanic regions [*Menzel et al.*, 1998]. Derived products generated operationally by NOAA/NESDIS, include clear-sky radiances, atmospheric temperature (T) and moisture (Q) profiles, TPW, cloud-top pressure, and water-vapor atmospheric motion vectors. Selected additional Sounder products, including total column ozone, are also produced at the Cooperative Institute for Meteorological Satellite Studies (CIMSS) at the University of Wisconsin-Madison (UW). Applications of the GOES Sounder products include: nowcasting and forecasting of weather events, assimilation of cloud products into regional numerical forecast models, and monitoring of T and Q changes in the pre-convective environment [*Schmit et al.*, 2002].

[3] To improve short-term severe storm nowcasting, knowledge of T and Q distributions both spatially and temporally is very important. In an effort to provide better moisture fields for severe storm nowcasting, an improved physical retrieval algorithm has been developed and applied to the GOES-12 Sounder measurements at CIMSS; it will build upon the legacy version [*Ma et al.*, 1999] that has been successfully applied to GOES-8/9/10/11/12 measurements [*Schmit et al.*, 2002].

[4] In general, two types of algorithms are used for sounding retrievals: statistical retrievals, which are generally a linear regression [*Goldberg et al.*, 2003; *Li et al.*, 2000], and physical retrievals [*Susskind et al.*, 1984; *Ma et al.*, 1999; *Eyre*, 1989; *Li et al.*, 2000]. For the GOES Sounder regression retrievals, forecast T and Q profiles are usually included as predictors to assist the regression due to the limited profile information contained in 18 IR spectral bands. The physical retrieval algorithm is a more commonly used method on the current GOES Sounder. During early development of the physical algorithm, linearization was used to solve the unknowns simultaneously [*Smith*, 1983; *Hayden*, 1988]. But it is somewhat limited since the radiative transfer equation (RTE) is highly nonlinear to T and Q. In recent years, nonlinear physical retrieval algorithms have been developed [*Smith*, 1983; *Susskind et al.*, 1984; *Ma et al.*, 1999; *Eyre*, 1989; *Li et al.*, 2000] for GOES Sounder data processing. Both the linear and nonlinear algorithms depend highly on the accuracy of the first guess.

[5] Building on the approach of *Ma et al.* [1999], the improved physical retrieval algorithm, presented in the next section, updates almost all major parts of the algorithm. TPW retrievals from both the legacy and the improved versions are compared with MWR measurements of atmospheric moisture. The application of improved sounding products on short-term severe storm nowcasting is presented.

2. Improved Retrieval Algorithm

[6] The retrieval algorithm includes the regression technique that serves as the first guess for the physical iterative algorithm.

2.1. Regression Algorithm

[7] For better accuracy, a linear regression procedure is used to generate the first guess for the physical iterative approach instead of the numerical weather prediction model forecast. The main predictors for the regression include: 1) the brightness temperatures (TB) (including the quadratic terms of TB); 2) the forecast profiles; 3) surface T and Q observations; and 4) other variables. The training database

[1]Cooperative Institute for Meteorological Satellite Studies, University of Wisconsin-Madison, Madison, Wisconsin, USA.
[2]Center for Satellite Applications and Research, National Environmental Satellite, Data, and Information Service, NOAA, Camp Springs, Maryland, USA.

Copyright 2008 by the American Geophysical Union.
0094-8276/08/2007GL032797$05.00

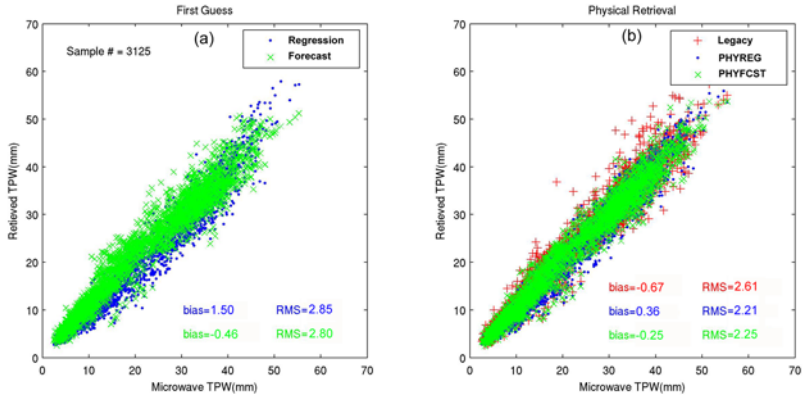

Figure 1. TPW retrievals versus microwave-measured TPW at the SGP CART site from June 2003 to May 2005. The x-axis presents MWR measured TPW, and the y-axis presents (a) the first guess and (b) different physical retrievals applied to the GOES-12 Sounder. PHYREG and PHYFCST are the improved physical retrievals using regression and GFS forecast as first guess respectively.

is a match-up database containing temporally and spatially collocated radiosonde observations (RAOBs), the GOES-12 Sounder TB measurements and the NCEP GFS model forecast profiles (the RAOB/GOES/GFS match-up database) from June 2003 to September 2004 over the continental United States (CONUS).

2.2. Physical Algorithm

[8] The nonlinear physical algorithm used in this study is very similar to that of *Ma et al.* [1999]. The main updates to the algorithm are given below; for further information, please refer to equations (8), (12) and (16) of *Ma et al.* [1999].

[9] 1) The first guess. Regression-retrieved T and Q profiles are used instead of the forecast profiles. Surface emissivities are also improved with a synthetic regression-based surface emissivity scheme derived from SeeBor training database [*Seemann et al.*, 2008].

[10] 2) The error covariance matrix of the retrieval parameters. It has been found that this term affects the retrieval precision greatly; the better the covariance matrix represents the first guess errors, the better the final optimal retrieval. In the legacy algorithm, *Ma et al.* [1999] used a correlation coefficient matrix instead of a real covariance matrix for the first guess. In this study, two covariance matrices were calculated using the RAOB/GOES/GFS match-up database: one for the regression and the other for the forecast. The biggest advantage of using the real covariance matrix is that no regularization parameter is actually needed for convergence.

[11] 3) The observed radiances. A new radiance bias adjustment scheme is applied using the RAOB/GOES/GFS match-up database to reduce the bias between calculated and observed radiances. Additionally, clear-sky radiances are spatially averaged; the averaging area increases for spectral bands not sensitive to the lower atmosphere (this is sometimes referred as inverted cone averaging).

[12] 4) The calculated radiances. The Pressure-Layer Fast Algorithm for Atmospheric Transmittance (PFAAST) models [*Hannon et al.*, 1996] is applied to calculate the GOES-12 Sounder radiances. PFAAST is based on the line by line radiative transfer model (LBLRTM) version 8.4 [*Clough and Iacono*, 1995] and the high-resolution transmission molecular absorption database-2000 (HITRAN-2000) [*Rothman et al.*, 1992] with updates (aer_hitran_2000_updat_01.1).

3. Validation

[13] Atmospheric moisture typically has more variability than temperature in both space and time. It is also more complicated than temperature in atmospheric thermodynamic processes due to latent heat. Over CONUS, the GFS Model forecast has been found to predict the temperature well, but moisture less well. Therefore, this validation focuses on the moisture products, particularly the TPW which can accurately be measured from ground-based instruments.

[14] Every five minutes, a microwave radiometer at the SGP CART site at Lamont, OK (36° 37′N, 97° 30′W) provides measurements of column-integrated amounts of water vapor (http://www.arm.gov/instruments/instrument.php?id = mwr). This microwave-measured TPW, with accuracy of 0.7 mm, is excellent for GOES-12 Sounder retrieval validation. The time coverage included in this work is from June 2003 to May 2005 with sample size of 3125. The closest GOES-12 Sounder Field-of-View (FOV) to Lamont is chosen as the collocated FOV. A 3 by 3 average method is used to filter out the random noise in the radiances.

[15] Figure 1 shows the scatter plots between MWR measured and GOES-12 Sounder retrieved TPW. Both the legacy and the improved physical algorithm compare better than the first guess. The RMS is reduced after the physical retrieval. The legacy version (forecast was used as first guess) reduces RMS by 0.19 mm while bias is increased by 0.21 mm. The physical retrieval algorithm using regression as first guess (PHYREG) reduces the bias by 1.14 mm and RMS by 0.64 mm, and the physical retrieval algorithm using forecast as first guess (PHYFCST) reduces the bias by 0.21 mm and RMS by 0.55 mm. Although the two first guesses have about the same precision of 2.8 mm in RMS, the RMS of the improved physical retrievals (both PHYREG and PHYFCST) is about 0.4 mm smaller than the legacy physical results. This indicates the improved physical algorithm performs better than the legacy version.

Also, the improved physical retrieval shows a smaller bias (0.36 mm for PHYREG and −0.25 mm for PHYFCST) than the legacy physical results (−0.67 mm), which again demonstrates the superiority of the improved physical algorithm.

[16] The regression retrieval has a much larger bias (1.50 mm) and slightly larger RMS (2.85 mm) than the forecast (−0.46 mm of bias and 2.80 mm of RMS) in Figure 1a. This is likely because of the failure to detect thin, low or broken clouds prior to the retrieval. The regression coefficients are derived under clear-sky conditions and are not suitable for cloudy situations. When the clouds are thick, the regression cannot provide a reasonable profile and the retrieval is flagged as a failure. However, when the clouds are thin, low or broken, the regression is able to return a reasonable profile albeit containing a bias, which increases the regression guess RMS. The larger bias and RMS do not affect the physical retrieval very much: PHYREG (2.21 mm) shows slightly better results than PHYFCST (2.25 mm) in terms of RMS. Therefore, in the next section, the physical algorithm takes the regression (PHYREG) as first guess.

4. Application to Short-Term Severe Storm Nowcasting

[17] For short-term severe storm nowcasting, the GOES Sounder DPI with hourly temporal resolution and nominal 10 km spatial resolution can prove to be very useful [*Menzel et al.*, 1998]. Two supercell cases are presented to demonstrate how the GOES Sounder products available via the improved physical algorithm might assist the forecasters on short-term severe storm nowcasting. In the first tornadic storm, the lifted index (LI) is used to depict the potential convective environment surrounding a supercell before and during its development. In the second hail storm case, different air masses around a supercell are identified, especially the one supplying low-level moisture into the supercell.

4.1. Tornadic Storm at Eagle Pass, Texas on 24 April 2007

[18] The LI, a measurement of atmospheric instability, is the difference between the temperature at 500 hPa and the temperature an air parcel will have by lifting from the surface to 500 hPa. A positive value indicates a stable atmosphere, in which convection is unlikely. A LI of between 0 and −3 (degree Celsius) indicates that the air is marginally unstable and unlikely to lead to severe thunderstorms. Values between −3 and −6 indicate moderately unstable conditions. Values between −6 and −9 are found in very unstable regions. LI values less than −9 reflect extreme instability. The chances of a severe thunderstorm are best when LI is less than or equal to −6.

[19] At approximately 0000 UTC on 25 April 2007, a tornado that had originated in far northeast Mexico passed through the Eagle Pass area of Texas (the green X in Figure 2m, n and o). This EF-3 tornado killed 10 people in Mexico and the United States with another 120 injured. While forecasting such a fatal tornado remains challenging to forecasters and regional modelers, the GOES-12 Sounder DPI of LI could provide useful information to forecasters during such an event.

[20] Figure 2 shows the time series of the derived LI imagery. Non-cloudy areas are filled with LI values, with different colors representing different levels of severity. Cloudy areas are filled with 11 μm TB; colder TB are reflected in brighter grey shades. From the top to bottom is 20, 21, 22 and 23 UTC on April 24. The actual local scanning time is about 10 minutes after the label time. From the left to the right is GFS forecast, legacy physical retrieval and PHYREG.

[21] One of the difficulties in forecasting such a supercell is the short lifetime of the whole system (typically just a few hours). It is very difficult for forecasters to predict where and when a supercell is going to form. In this case, it will be demonstrated that the LI values in the vicinity of weather systems are well correlated with the outbreak and the development of the systems. At around 19 UTC, neither the 11 μm imagery (no cold clouds) nor the LI DPI imagery (not shown here) indicate that a severe convective storm will be developing soon. However, one hour later, the LI DPI imagery (and hence the PHYREG retrievals) change dramatically from "marginally unstable" to "moderately unstable" and "very unstable" (the red region among the yellow area in Figure 2c). This indicates a more favorable pre-convective environment. The same degree of convective potential (in terms of coverage) is not seen on either the GFS forecast or legacy retrieval DPI imagery at 20 UTC (Figures 2a and 2b). The GOES Imager animation (http://www-angler.larc.nasa.gov/armsgp/g8usa.html/) shows the outbreak of the supercell occurring immediately prior to 2015 UTC. Note that the cloud top TB was less than 220 K in 11 μm at 21 UTC.

[22] During the next several hours, the supercell grew rapidly, and the center of the cell moved southeast along the border. Compared with the GFS forecast, the legacy retrievals reveal increasing areas of instabilities surrounding the supercell; the improved retrievals are even more extended and pronounced. Figure 2o shows three areas of large negative LI values. To the south of the supercell, the instabilities ensured the continuous growth of the supercell. To the northwest of the supercell, the instabilities initialized (between 22 and 23 UTC) and maintained another convective storm to the north of the supercell. To the west of the supercell, the instabilities initialized (between 01 and 02 UTC, not shown) and maintained the third convective storm. Not shown here are the instabilities that returned to normal values during the post-stage of the convective storms.

4.2. Wisconsin Hailstorm on 14 April, 2006

[23] From approximately 0140 UTC to 0400 UTC on 14 April 2006, a severe thunderstorm moved across southern Wisconsin. The estimated loss of property was about 160 million dollars, most of which was caused by 1 to 4 inch diameter hail and downburst winds.

[24] In order to identify the low-level moisture, which is an important factor for severe thunderstorm development, we separate the air mass into 10 different classes (only 4 clear-sky classes are shown in Figure 3a) with a clustering method [*Li et al.*, 2007] using the GOES-12 Sounder IR channels 1–15. Then the improved physical retrieval is performed on the clear-sky average of each class. The advantage is an improved signal-to-noise ratio. To represent

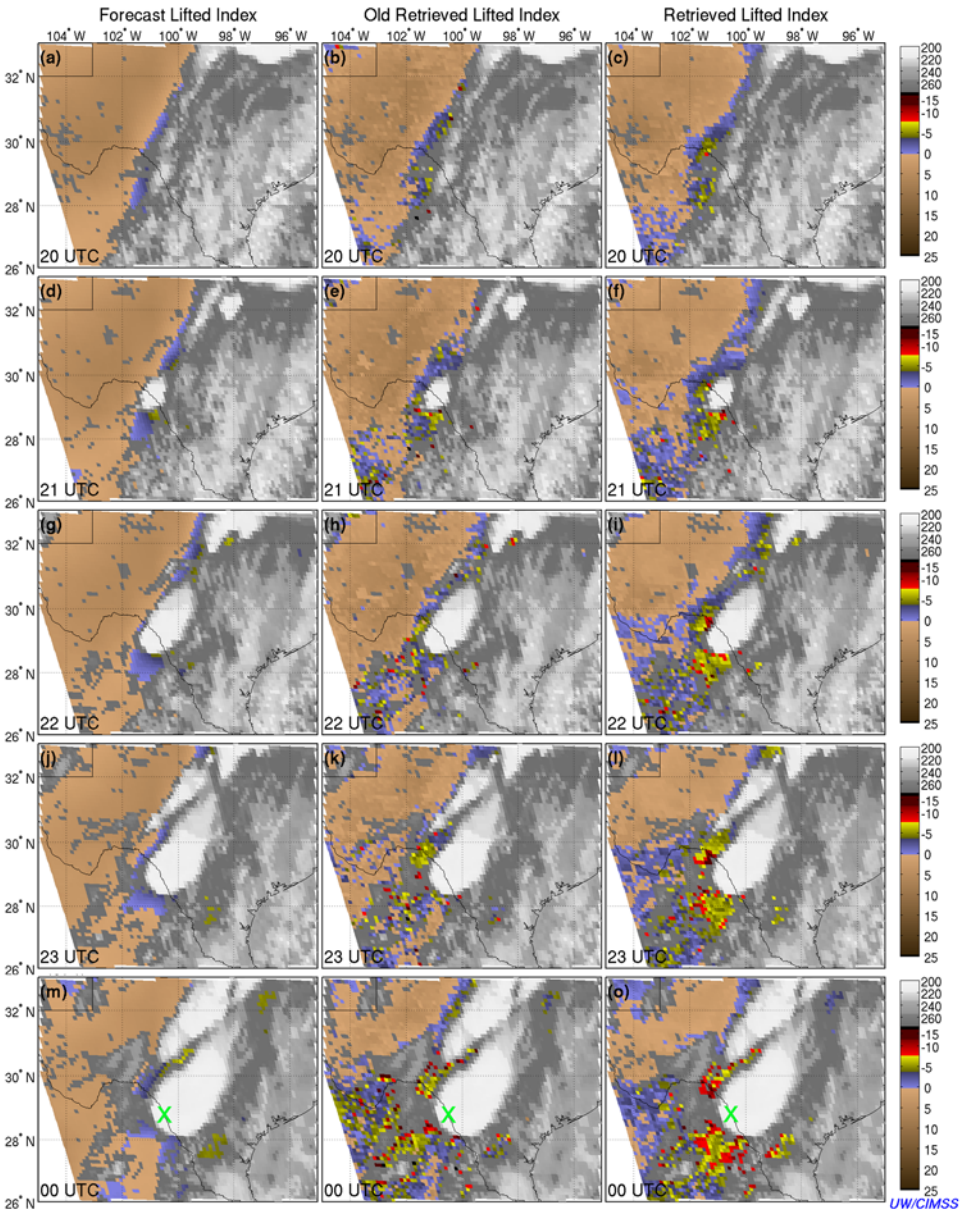

Figure 2. Time series of LI DPI imagery on 24 April 2007. From top to bottom is 20, 21, 22, 23 and 00 UTC. From the left to the right is GFS forecast, the legacy retrieval and PHYREG. A tornado touched down near Eagle Pass, Texas (the green X along the Texas/Mexico border within the supercell in the bottom three plots) around 0000 UTC.

the environment around the supercell, only FOVs close enough to the supercell are used. The black rectangle in Figure 3a shows the area under consideration.

[25] Figure 3 shows the results for 00 UTC, 2 hours after the outbreak in Iowa. This time was selected for two reasons: 1) the spatial distribution of the different air masses remained the same except for some eastward propagation; 2) the operational NOAA weather chart and the ECMWF (European Centre for Medium-Range Weather Forecasts) analysis field from 00 UTC help evaluate the results. The supercell is clearly identified as the black X in Figures 3a and 3b. Figures 3d–3f are the relative humidity (RH) difference profiles compared with the light blue class. All show the dry-to-wet gradient from west to east. However, they differ in the lower atmosphere between 900 and 1000 hPa; both the brown class from the retrieval (Figure 3e) and ECMWF analysis (Figure 3f, 0.25 degree spatial resolution) are well separated from other classes (about 25 % more RH than others), perhaps indicating it is the main path of moisture transported into the growing supercell, as suggested by the southerly surface winds over this area (http://www.spc.noaa.gov/obswx/maps/). This 25 % RH difference along with the absolute values of RH as large as 80 % (not shown) ensures the quick and continuous growth of the supercell, while the GFS forecast shows only an RH difference of about 10–15%.

[26] The temperature gradients in the vicinity of the supercell are also important. Figure 3c shows the profiles of the retrieved temperature differences compared to the light blue class. The temperatures below 650 hPa show a warm-to-cold gradient from west to east. This gradient, especially between the light blue and the brown, is a key

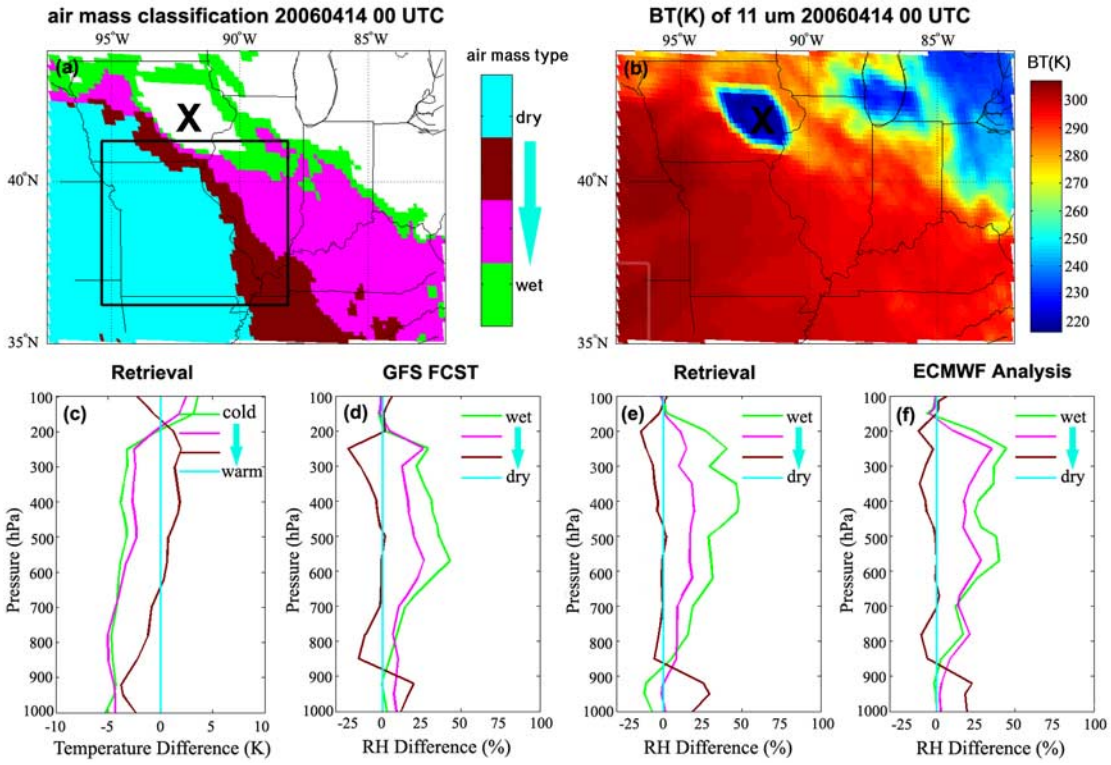

Figure 3. GOES-12 Sounder classification of air masses and their associated moisture structures at 00 UTC 14 April 2006: (a) classification of air mass; (b) 11 μm brightness temperature; (c) profiles of temperature difference of different air masses compared with the light blue class; and profiles of relative humidity differences compared with the light blue classes from (d) the GFS forecast, (e) the improved retrievals, and (f) the ECMWF analysis. Black X denotes the supercell, while the black rectangle encompasses the region used to compute the average of each class.

factor for the supercell to grow. The dry and hot air mass between 700 and 900 hPa (see Figure 3c) blows eastwardly (http://www.spc.noaa.gov/obswx/maps/), climbing up to the relative cool and moist air mass, forming a cap. This inversion cap inhibits the instability from being released until reaching the supercell, maintaining the low-level moisture path.

5. Summary

[27] By using a realistic error covariance matrix of retrieval parameters, an improved fast forward RTM, a radiance bias adjustment scheme, inverted cone clear-sky observed radiance averaging, a first guess from regression, and an improved surface emissivity scheme, the improved physical retrieval algorithm is able to produce better retrievals of temperature and moisture profiles from GOES-12 Sounder radiances than the previous legacy algorithm, which is currently used in CIMSS routine GOES Sounder data processing. The improved physical retrieval algorithm betters the retrieval of TPW by 0.4 mm over the old legacy version when the retrievals are compared with SGP CART site microwave radiometer TPW measurements. A case study of a deadly tornadic supercell at Eagle Pass, Texas on 24 April 2007 reveals that the improved physical retrieval is able to identify the pre-convective environment better than the previous legacy retrievals. Another supercell case on 14 April 2006 demonstrates that the improved physical algorithm is able to detect low-level moisture. These hourly products provide information that should help forecasters estimate the further development of the current weather system.

[28] The improved algorithm is now being tested at CIMSS and will be transferred into operations under the support of GOES-PSDI (Product System Development and Integration). The products, including the DPI of TPW, LI and skin temperature, will be distributed through AWIPS (the Advanced Weather Interactive Processing System).

[29] **Acknowledgments.** The authors would like to thank Harold M. Woolf for providing the 101-level GOES Sounder radiative transfer model. This program is supported at CIMSS by NOAA GIMPAP program NA06NES4400002 and GOES-R program NA07EC0676. The views, opinions, and findings contained in this report are those of the authors and should not be construed as an official National Oceanic and Atmospheric Administration or U.S. Government position, policy, or decision.

References

Clough, S. A., and M. J. Iacono (1995), Line-by-line calculations of atmospheric fluxes and cooling rates: 2. Applications to carbon dioxide, ozone, methane, nitrous oxide and the halocarbons, *J. Geophys. Res.*, *100*, 16,519–16,535.

Eyre, J. R. (1989), Inversion of cloudy satellite sounding radiances by nonlinear optimal estimation. I: Theory and simulation for TOVS, *Q. J. R. Meteorol. Soc.*, *115*, 1001–1026.

Goldberg, M. D., Y. Qu, L. M. McMillin, W. Wolf, L. Zhou, and M. Divakarla (2003), AIRS near-real-time products and algorithms in support of operational numerical weather predication, *IEEE Trans. Geosci. Remote Sens.*, *41*(2), 379–389.

Hannon, S., L. L. Strow, and W. W. McMillan (1996), Atmospheric infrared fast transmittance models: A comparison of two approaches, *Proc. SPIE Int. Soc. Opt. Eng.*, *2830*, 94–105.

Hayden, C. M. (1988), GOES-VAS simultaneous temperature-moisture retrieval algorithm, *J. Appl. Meteorol.*, *27*, 705–733.

Li, J., W. Wolf, W. P. Menzel, W. Zhang, H.-L. Huang, and T. H. Achtor (2000), Global soundings of the atmosphere from ATOVS measurements: The algorithm and validation, *J. Appl. Meteorol.*, *39*, 1248–1268.

Li, Z., J. Li, T. J. Schmit, W. P. Menzel, and S. A. Ackerman (2007), Comparison between current and future environmental satellite imagers on cloud classification using MODIS, *Remote Sens. Environ.*, *108*, 311–326.

Ma, X. L., T. J. Schmit, and W. L. Smith (1999), A nonlinear physical retrieval algorithm—Its application to the GOES-8/9 sounder, *J. Appl. Meteorol.*, *38*, 501–513.

Menzel, W. P., F. C. Holt, T. J. Schmit, R. M. Aune, A. J. Schreiner, G. S. Wade, G. P. Ellrod, and D. G. Gray (1998), Application of the GOES-8/9 soundings to weather forecasting and nowcasting, *Bull. Am. Meteorol. Soc.*, *79*, 2059–2077.

Rothman, L. S., et al. (1992), The HITRAN molecular database: Editions of 1991 and 1992, *J. Quant. Spectrosc. Radiat. Transfer*, *48*, 469–507.

Schmit, T. J., W. F. Feltz, W. P. Menzel, J. Jung, A. P. Noel, J. N. Heil, J. P. Nelson, and G. S. Wade (2002), Validation and use of GOES sounder moisture information, *Weather Forecasting*, *17*, 139–154.

Seemann, S. W., E. E. Borbas, R. O. Knuteson, G. R. Stephenson, and H.-L. Huang (2008), Development of a global infrared land surface emissivity database for application to clear-sky sounding retrievals from multi-spectral satellite radiance measurements, *J. Appl. Meteorol. Climatol*, in press.

Smith, W. L. (1983), The retrieval of atmospheric profiles from VAS geostationary radiance observations, *J. Atmos. Sci.*, *40*, 2025–2035.

Susskind, J., J. Rosenfield, D. Reuter, and M. T. Chahine (1984), Remote sensing of weather and climate parameters from HIRS2/MSU on TIROS-N, *J. Geophys. Res.*, *89*, 4677–4697.

S. A. Ackerman, J. Li, Z. Li, W. P. Menzel, and J. P. Nelson III, Cooperative Institute for Meteorological Satellite Studies, University of Wisconsin-Madison, 1225 West Dayton Street, Madison, WI 53706, USA. (zhenglong.li@ssec.wisc.edu)

J. Daniels and T. J. Schmit, Center for Satellite Applications and Research, NESDIS, NOAA, 5200 Auth Road, Camp Springs, MD 20746, USA.